Hindawi
Journal of Mathematics
Volume 2022, Article ID 2281202, 12 pages
https://doi.org/10.1155/2022/2281202

Research Article

Research on Forest Carbon Sequestration Based on FSC Model and DeepAR Algorithm

Yin-di Xu

School of Statistics and Applied Mathematics, Anhui University of Finance and Economics, Bengbu 233030, China

Correspondence should be addressed to Yin-di Xu; 20193134@aufe.edu.cn

Received 27 March 2022; Accepted 20 April 2022; Published 19 May 2022

Academic Editor: Hassan Raza

Forestry resources play an irreplaceable role in solving the problem of climate change. Forest managers to find a balance between carbon sinks and forest products, decisions must therefore take into account many aspects of forest value. This paper clarifies that forest carbon sequestration is mainly influenced by three aspects: human, climate, and nonclimatic physical factors, constructs a model for estimating the carbon sequestration rate of forest ecosystems based on forest age and the logistic growth equation, and combines human behaviour and climate influencing factors to make comprehensive corrections to the carbon sequestration rate of forest ecosystems per unit area. A model for calculating the carbon sequestration rate over time in a forest system was developed, which combined with the DeepAR Algorithm to obtain carbon sequestration. Then, this paper then assesses the various values of the forest, dividing the 25 factors affecting forest value assessment into five indices to establish a model of the forest ecosystem value assessment system for application to forest value assessment under different conditions. After determining the index system, we use the EWM-CVM to integrate the indexes into the value index based on the forest ecosystem to propose a management plan. And the PSO-BP algorithm is used to determine the transition point for forest management in order to optimise the ecological value of the forest.

1. Introduction

In recent years, the emission of carbon dioxide and other greenhouse gases in the process of production and living has increased dramatically [1].Forestry resources play an irreplaceable role in solving the problem of climate change. The main ecological function of forests is to absorb carbon dioxide and release oxygen [2–6].This is conducive to reducing greenhouse gases in the atmosphere. However, if climate change is to be effectively addressed, carbon sequestration is needed. Forest management strategies with appropriate logging are conducive to carbon sequestration. For forest managers to find a balance between carbon sinks and forest products, decisions must therefore take into account many aspects of forest value.

In this paper, an FCS model based on classical logistic equations of forest age and biomass was developed to explore the carbon cycle between vegetation, litter and soil. In order to consider the effects of herbivores, fire and water erosion on the carbon sink, the results of a combined analysis were used, considering 58% of the ideal state as the result, assuming that the model excludes the interference of human behaviours and climate effects. Forest carbon sequestration is one of the main ways to mitigate climate change, and forests, as the mainstay of terrestrial ecosystems, are the largest carbon reservoir in the system. Forest carbon sinks are also one of the most cost-effective ways to combat climate change. Forests sequester carbon using natural processes that do not require high costs and at the same time have ecological benefits such as protecting biodiversity, conserving water and preventing wind and sand.

2. Literature Review

In recent decades, scientists have carried out a great deal of research on climate change and its effects. The wide range of research and the variety of research methods all indicate that the effects of climate change are very complex, affecting

almost all natural and socio-economic systems. The impact of climate change has a certain transmissibility, which can be reflected in natural systems and transmitted to social and economic systems [7].

In order to cope with the increasingly severe global climate change situation, the IPCC calls on countries to reduce carbon emissions and promote carbon neutrality, and strive to achieve net zero emissions of carbon dioxide. In order to achieve this goal, in addition to large-scale implementation of renewable energy substitution and tapping the potential of energy saving and carbon reduction technologies such as hydrogen production from renewable energy, it is also necessary to vigorously develop carbon capture and storage technologies [8–14].This shows the role of "carbon sequestration" in addressing the impacts of climate change. The ability of carbon management in forest management plans to effectively manage carbon emissions led to the birth of the International Carbon Management Partnership, which sets guidelines for forest managers around the world.

As the composition, climate, population, interests and values of forests vary greatly around the world, different management plans need to be formulated according to different situations. Only by considering various factors can the forest management plans thus obtained be practical. Therefore, it is necessary to establish a decision-making model to determine the specific forest management plan in order to solve the impact of climate change.

3. Assumptions and Symbols

In response to the problems studied in this article, to better establish the model without affecting the accuracy of the model, we have made the following assumptions: (i) The development from the current state to the proposed state is stable. Sudden changes can be ignored because of their rareness; (ii) Excluding the impact of uncontrollable factors on the data, such as fires, planetary impacts on forests, etc; (iii) The climatic impact on NPP variations can be estimated by RC on a location basis in an LVSA zone; (iv) Statistics we collect from the website are actual and reliable; (v) Assuming that global climate change is consistent and that temperature and precipitation are important parameters in FCS models, however, under different global climate change scenarios, the estimates may contain a high degree of uncertainty, which may lead to uncertainty in forest carbon stock estimates. At the same time, the abbreviations and definitions mentioned in this article are shown in Table 1.

4. Forests Carbon Sequestration Model Based on the Logistic

4.1. Forests Vegetation Year in the FCS Model. Based on the classical logistic equation of forest age and biomass, the FCS model was established [15] to explore the carbon cycle among vegetation, litter, and soil. To consider the impacts of herbivores, fire, and water erosion on carbon sinks, we used the results of the integrative analysis conducted [16] and regarded 58% in the ideal state as the result. We assume that this model excludes the interference of human behaviour and climatic influences. With forest development, forest biomass gradually reaches a relative equilibrium state [17]. The annual growth rate of vegetation biomass can be simply defined by follows:

$$\frac{\mathrm{d}B_t}{\mathrm{d}t} = v_0\left(1 - \frac{B_t}{B_{\max}}\right)B_t, \tag{1}$$

$$B_t = \frac{B_{\max}}{1 + \left(\left(B_{\max}/B_{t_0}\right) - 1\right) \times e^{-v_0 \times (t - t_0)}}, \tag{2}$$

where B_t is the forest vegetation biomass (Mg ha^{-1}); V_0 is the intrinsic growth rate, representing the maximum growth rate when vegetative growth is not limited by the environment, nutrients, or disturbances; $B_{\max}$ is the maximum vegetation biomass under the mature forest scenario (Mg ha^{-1}); $1 \rightarrow B_t/B_{\max}$ represents the fractional deficiency of the current biomass to its saturation level; and t is the forest age (year).Three key parameters were well defined or validated using the field data at a large scale [18].

In this study, we considered 80 years as the age of a mature forest and collected vegetation biomass data of mature forests from the public databases. Vegetation biomass in mature forests was calculated by MAT and MAP using:

$$B_{\max}(\mathrm{MAT}, \mathrm{MAP}) = 3442.914 \times \frac{0.05 + \exp(0.000158 \times \mathrm{MAP})}{1 + \exp(-0.037 \times (\mathrm{MAT} - 95.606))} + 33.128. \tag{3}$$

In equation (6), MAT is the mean annual temperature (°C), and MAP is the mean annual precipitation (mm).The Miami model considered MAT and MAP to be key factors for vegetation productivity.

dB_{Miami} is the annual productivity estimated by the modified Miami model (Mg ha^{-1} yr^{-1}) in the following equation:

$$\mathrm{d}B_{\mathrm{Miami}} = 30 \times \sqrt{\frac{1 - \exp(-0.00031 \times \mathrm{MAP})}{1 + \exp(0.12345 - 0.2606 \times \mathrm{MAT})}}, \tag{4}$$

$$v_0 = \frac{\mathrm{d}B_{\mathrm{Miami}}}{B_t} = 0.081 \times \exp(0.038 \times \mathrm{MAT}) + 0.065 \times \ln(\mathrm{MAP}) - 0.38. \tag{5}$$

4.2. Soil Carbon Cycles in the FCS Model. The soil organic carbon (SOC) level in forests is the result of the combined effects of the humification and mineralization processes [19].When the factors of forests are relatively stable, the humification and mineralization processes will tend to balance the SOC level, as shown in

$$\frac{\mathrm{d}C_t}{\mathrm{d}_t} = I_t - k_2 C_t, \tag{6}$$

where C_t is the SOC density (Mg C ha^{-1}) and I_t is the annual input of SOC (Mg ha^{-1} a^{-1});

Table 1: Notations.

Symbols	Definition
FV	Forest value, EST
SC	Socio-economic conditions index
IV	Indirect value index
V_i	The coefficient of variation of the index i
θ_i	The standard deviation of the index i
Tiq	The desired outputs of the network under the network weights Oiq
FCS	Forest carbon sequestration
NPP	Net primary productivity
FV	Forest value, EST
SC	Socio-economic conditions index
IV	Indirect value index
V_i	The coefficient of variation of the index i

$$I_t = h(k_1 L_t). \tag{7}$$

L_t is the litter content (Mg ha^{-1}); k_1 is the litter decomposition coefficient; k_2 is the SOC decomposition rate (a^{-1}); and h is the decay coefficient (0.3).

$$C_t = \frac{I_t}{k_2} - \left(\frac{I_t}{k_2} - C_{t_0}\right)\exp\left(-k_2(t - t_0)\right). \tag{8}$$

During the development of the FCS model, we used the multi-source investigation data over the past few decades to optimise the key parameters.

4.3. Forest Carbon Sequestration of Human and Climatic Factors. The net carbon flows from natural and mixed forests published by UNESCO are shown in Figure 1. Spatial differences in forest carbon sequestration will be entirely attributable to human influence once the differential effects of climate and non-climate on forest carbon sequestration are excluded. We use net primary productivity(NPP) to express the carbon sequestration capacity of forests in terrestrial ecosystems. Our main objective is to assess how much carbon can realistically be obtained from global terrestrial vegetation by renewing humans alone, without changing land use and land cover or forest biomes. We use publicly available time series datasets to analyse the carbon gap. The data source is from Google Earth Engine (GEE) [20]. Data pre-processing and analysis was also performed on the GEE computing platform. There are four sets of data sources involved, namely climate-related variables, (non-climate) physical environment variables, country productivity and world population. These data sets, if not at the *500m scale*, were uniformly resampled to a resolution of *500m*. Region segmentation of homogeneous natural environments to detach non-climate impacts on NPP variation. Region segmentation is performed by over-laying the layers of landform (L), vegetation type (V), soil type (S)and tree age(A) characteristics to derive homogeneous zones, known as homogeneous LVSA zones.Over the pixels within the same LVSA zone, the impact from the non-climate environmental factors on the internal NPP variation is uniform. Thus, any NPP variation within an LVSA zone is attributed to varied climatic and human impacts only [21].

The NPP dataset provides a direct indicator of the carbon sequestration of forests, and reflects the spatial and temporal variability of forests carbon sequestration [22].We assume that the Miami model can be applied to measure the relative impact on NPP from climate variations in an LVSA zone. The Miami model is used to assess the climate impact on PNPP, which takes the form

$$PNPP = \lambda \times \min\left\{\frac{3000}{1 + e^{1.315 - 0.119t}}, 3000 \times \left(1 - e^{-0.000664p}\right)\right\}, \tag{9}$$

where t is the annual average temperature (°C), p is the annual precipitation (mm), and λ is a conversion coefficient (0.50 for woody ecosystems and 0.45 for herbaceous) that converts dry matter to carbon unit (gCm^{-2}yr^{-1}).

For discriminating the varied climate impact on NPP in an LVSA zone, where *PNPP(i, g)* is PNPP at i in g, $PNPP_{mean}$ (g) is the mean PNPP of all the locations in g:

$$RC(i, g) = PNPP(i, g) - PNPP_{mean}(g). \tag{10}$$

The climatic and human impact determine the NPP variations across an LVSA zone characterized by the identical landform, forests cover, and soil properties. Climate-rectified NPP (NPP_{CR}) at location i in g can be derived using the function

$$NPP_{CR}(i, g) = NPP(i, g) - RC(i, g). \tag{11}$$

$NPP_{CR}(i,g)$ is the rectified NPP at location i in g after the climatic impact on NPP is removed. When spatial variations of NPP_{CR} within an LVSA zone are observed, it is attributed to human influence, i.e., the difference in land-management practices (LMPs).

These best LMPs can be deemed to be the optimal BLMPs under similar environmental conditions over this LVSA zone. A window size specifies a local neighborhood surrounding given location in which the NPP_{CR} values at all the locations with the identical LVSA in this window are taken as input to compute the NPP_{CR}^{final}. To decide the window size, a stratified random selection approach is taken to sample 5000 points in the vegetated land with the sample size weighted by the area of each of the biome types [23].

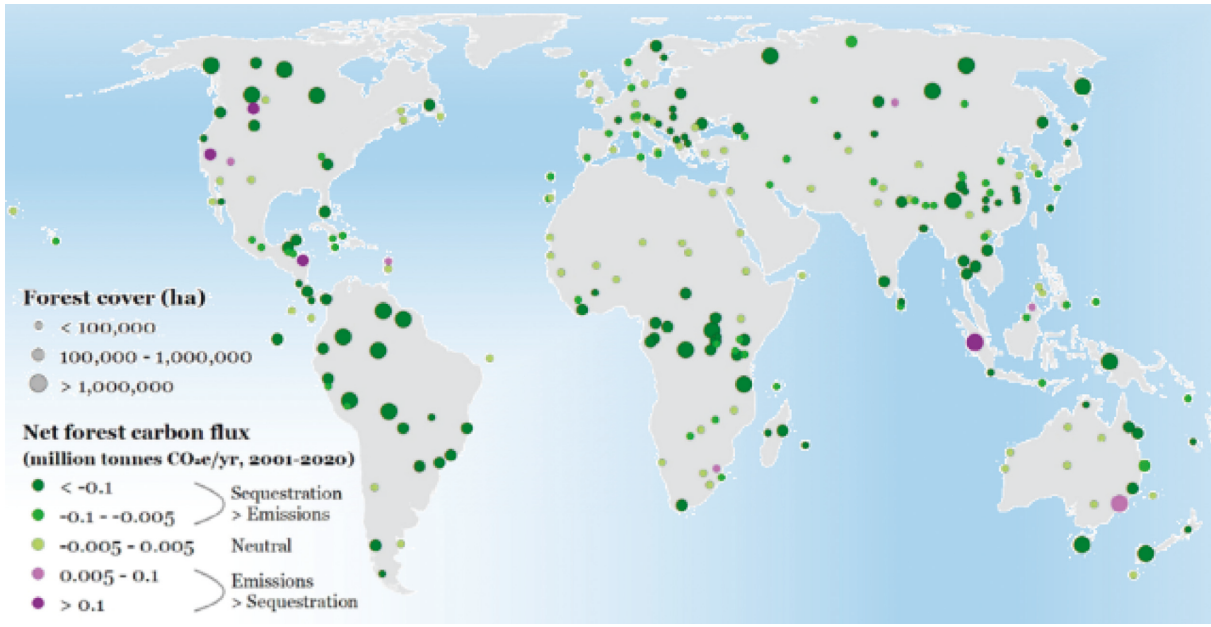

Figure 1: Net carbon flows from natural and mixed forests published by UNESCO.

As can be seen from Figure 2, the horizontal axis represents the distance and the vertical axis represents the amount of carbon sequestered, which presents a relatively stable stage when the distance is over *20 km* from the piecewise linear function fitting. Hence, the carbon sequestration at location i is computed as the difference between the current NPP_{CR} and the NPP_{CR}^{final} within the *20 km* window in the environmentally homogeneous zone:

$$C_i = \max\left(0, NPP_{CR}^{\text{final}} - NPP_{CR}^{i}\right). \tag{12}$$

The candidate of BLMPs for a location is decided by referring to the LMPs within the distance-constrained local window that boast identical environmental contexts but exhibit a higher level of carbon sequestration (i.e., where NPP_{CR} NPP_{CR}^{final}).

5. Optimal Assessment of Forest Value Benefits

5.1. Index Selection

5.1.1. Ecosystem Service Types. They can be divided into eight categories: (X1,X2,X3,X4,X5, X6,X7,X8), forest fruit products, water harvesting, carbon sequestration and oxygen release, air purification, forest recreation, biodiversity conservation, soil conservation, and nutrient accumulation. The eight types of ecosystem services can be classified as follows: there are significant differences in value assessment results depending on the type of ecosystem service.

5.1.2. Vegetation Zones. There are eight types of vegetation zones: (X9,X10,X11,X12,X13,X14,X15,X16), cold temperate coniferous forests, temperate mixed coniferous forests, warm temperate deciduous broadleaved forests, subtropical evergreen broadleaved forests, tropical (seasonal) rainforests, temperate grasslands, temperate deserts, and alpine vegetation zones. The vegetation zones determine the natural environmental conditions for forest growth and influence the supply of ecosystem services [24].

5.1.3. Area Characteristics. Fundamental to the enhancement of forest eco-efficiency is the continuous growth of forest resources. The total value of ecosystem services in a certain region is the sum of the value of all service functions provided by ecosystems in the region, which varies with the quality, area, and type of ecosystems in the region.

(1) *Forest Area (X17).* As forest area increases, the value of forest ecosystem services increases with the increase in forest cover. At the same time, the value of ecosystem services may have a marginal effect as forest area increases.

(2) *Forest Abundance (X18).* It has the area of other forests within a *50 km* radius from the centre of the study area. When the surrounding forests provide the same type of ecosystem services as the study area, i.e., they are substitutes, the value of ecosystem services in the study area may decrease as the area of other forests increases; conversely, if they are complements, there may be a positive relationship between the value of ecosystem services in the study area and the area of other forests.

(3) *Railway Length (X19).* It has the length of the railway within a *50 km* radius from the centre of the study area. The construction of railways causes fragmentation of the landscape. Therefore, there may be a negative relationship between the value of ecosystem services and railway length. There may be a negative relationship between the value of ecosystem services and the length of the railway [25].

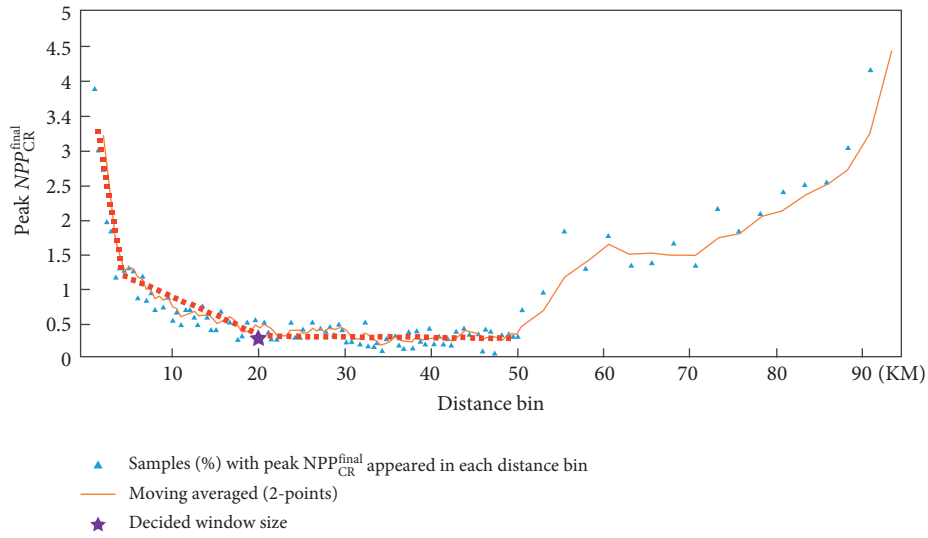

Figure 2: Samples with peak NPP_{CR}^{final} present in each distance bin.

5.1.4. Socio-Economic Conditions

(1) *Population (X20).* It means the number of people in an area with a radius of *50 km* from the centre of the study area. On the one hand, an increase in population means an increase in market and demand, which promotes the development and use of forest ecosystems; on the other hand, the concentration of population and the irrational use of resources increases the risk of environmental damage and causes the decline of ecosystems. Therefore, there is no definite a priori relationship between the value of ecosystem services and the number of people.

(2) *GDP Per Capita (X21).* GDP per capita is a reflection of the local economy and the standard of living of the people. Similar to the impact of population size, economic development can promote the use and conservation of forest ecosystems on the one hand, but can also lead to overexploitation of resources and ecological degradation on the other. There is therefore no definitive a priori relationship between the value of ecosystem services and GDP per capita.

(3) *Employment Benefits (X22).* Exploring the impact on the value of employment through the growth model of employment benefits from forest resources to enhance the sustainable use of forest resources, maintain ecological balance and sustainable socio-economic development.

5.1.5. Indirect Value. The social benefits of forests at the regional level are evaluated in three main areas: historical benefits, scientific and educational benefits, and cultural benefits *(X_{23}, X_{24}, X_{25})*.The scientific and educational benefits are considered in terms of education and research, the historical benefits are considered in terms of the value of famous and ancient trees, and the cultural benefits are mainly evaluated in terms of forest cultural products and forest practices.

5.2. Data Normalization. In our research, all index data firstly go through dimensionless treatment. According to the indicator data, we adopt the threshold method in linear dimensionless methods to make all the indicator data dimensionless [26].These 25 indicators can be classified into three types, cost-type index, benefit-type index, and moderate-type index. Among the three classes of indexes, the smaller the cost-type index is, the better the competitiveness degree of Ecosystems is. The benefit-type index is the opposite. The moderate-type index is better when it closer to a specific value. Due to the different contributions of the indexes, the three types of data are normalized in different ways [27].

(1) $Q_j\epsilon$ cost-type index. Let x_{ij} denote the $j-th$ index of the $i-th$, and it can be expressed as

$$x_{ij} = \frac{x_j^{\max} - x_{ij}}{x_j^{\max} - x_j^{\min}}, \tag{13}$$

where $x_j^{\max}$ is the most considerable value of Q_j, $x_j^{\min}$ is the smallest value of Q_j.

(2) $Q_j\epsilon$ benefit-type index.

$$x_{ij} = \frac{x_{ij} - x_j^{\min}}{x_j^{\max} - x_j^{\min}}. \tag{14}$$

(3) $Q_j\epsilon$ moderate-type index.

$$x_{ij} = \begin{cases} 1 - \dfrac{s_1 - d_{ij}}{\max\left\{\left(s_1 - d_j^{\min}, d_j^{\max} - s_2\right.\right.}, & d_{ij} < s_1, \\ 1, & d_{ij} = s_{1,} \\ 1 - \dfrac{d_{ij} - s_2}{\max\left\{s_2 - d_j^{\min}, d_j^{\min} - s_2\right\}}, & d_{ij} > s_1, \end{cases} \tag{15}$$

where s_1 is the best value of the indicator. Q.

5.3. Weight of Indicators

5.3.1. Entropy Weight Method. With the indicators defined above, we further determine the weights of these indicators, resulting in the combination of primary indicators. Recalling the entropy weight method (EWM) [28], we carry out the standardized treatment, making each variable optimal and worst value after alternation is 1 and 0, respectively. The evaluation indexes are $X_1, X_2, X_3, \ldots, X_k$, where $X_i = \{x_{i1}, x_{i2}, \ldots, x_{in}\}$.

After standardization, we introduce

$$p_{ij} = \frac{y_{ij}}{\sum_{i=1}^{n} y_{ij}}, \tag{16}$$

According to the concepts of self-information and entropy in the information theory, we can calculate the information entropy E_i of each evaluation indicator; hence we can obtain

$$E_i = -\ln\ (n)^{-1} \sum_{j=1}^{n} p_{ij} \ln\left(p_{ij}\right). \tag{17}$$

Based on the information entropy, we will further compute the weight of each evaluation indicator we defined before:

$$w_i = \frac{1 - E_i}{k - \sum_i E_i}, i = 1, 2, \ldots, k, \tag{18}$$

5.3.2. Coefficient of Variation Method. Furthermore, we apply the coefficient of variation method to weight these six indices and merge them into a comprehensive metric. Therefore, we will introduce the application of the coefficient of variation method briefly.

The coefficient of variation method (CVM) [29] utilizes the information from various indexes and achieves each Indicator weight through calculating, which shows an objective approach to give weight:

$$V = \frac{\theta_i}{z_i}\ (i = 1, 2, 3, 4, 5), \tag{19}$$

where V_i is the coefficient of variation of the index i, which can also be called as standard deviation coefficient, and θ_i means the standard deviation of the index i.And the $\boldsymbol{Z_{1\text{-}5}}$ separately means EST, VZ, AC, SC, and IV.

Then the weight of each index comes to us:

$$\frac{W_i = V_i}{\sum_{i=1}^{n} V_i}. \tag{20}$$

In this way, we are able to achieve the weight of each index without any subjective impression in Table 2.

$$\begin{aligned} FV = {} & W_1 \times EST + W_2 \times VZ + W_3 \\ & \times AC + W_4 \times SC + W_5 \times IV. \end{aligned} \tag{21}$$

6. Model Validation

6.1. CSRs in the Forests from 2010 to 2080. As can be seen from Figure 3, without considering extreme events and human interference, as expected, higher CSRs were observed in the young forests from 2010 to 2050,irrespective of the forests and soils, existing forests, and forestation level. However, 2050 to 2080 show a clear downward trend. The transition period lies between 2045 and 2055. The practical value (2010~2021) and predicted value(2021~2080) of CSRs in the forests from 2010 to 2080. The blue line is made by the method of FCS model, and the red dotted line is a fitting curve with a confidence interval of 0.95 [30].

The model was constructed using long-term datasets, which can suitably fit the relationship between forests biomass and forest age, but more long-term forest succession datasets are required to reduce the errors, considering the complexity of forest types and their wide distribution. At the establishment of the FCS model used here, some key parameters of the model were calibrated according to the investigated data of forest plots. Therefore, these representative local parameters made it better simulate the spatial C storage in forests to a large extent [31].

6.2. PSO-BP Algorithm Seeks Transition Points. The particle swarm algorithm can perform a rough search in the global scope to get an initial solution for BP relay, while the BP neural network algorithm can be used for gradient search with a strong refinement capability to perform a more careful search of the data. Here the transition point can be determined by using the algorithm for iterative search in the transition interval to get the final result. If the traditional gradient descent method is followed to find the optimum, this method often converges slowly and tends to fall into a local optimum [32]. In this paper, a combination of the PSO optimisation method and BP neural network is adopted to improve it. The connection weights and thresholds of the BP neural network are treated as elements of the position vector X of the particles in the particle swarm, and then the gradient descent method of the BP network is used instead of the particle swarm optimisation method to optimise the connection weights and thresholds of the network. The error in the output of this method comes mainly from the weights between the individual transmission channels.

The activation function chosen for this model is the Sigmoid function, which is given by

$$f(x) = \frac{1}{1 + e^{-x}}. \tag{22}$$

Net activation expression is given by

$$\text{net}_i = \sum_{j=1}^{n} w_{ij} x_j - \theta_i. \tag{23}$$

The input and output of each layer of neurons is calculated as follows:

Table 2: Index weights for forest value benefits.

Index (I)	Weight	Index (II)	Weight	Index (II)	Weight	Index (II)	Weight
		X_1	0.1340	X_4	0.0474	X_7	0.1476
Ecosystem service types	0.2657	X_2	0.1712	X_5	0.0276	X_8	0.2059
		X_3	0.1689	X_6	0.0974	EST	0.2657
		X_9	0.2046	X_{12}	0.1529	X_{15}	0.1535
Vegetation zones	0.2014	X_{10}	0.0418	X_{13}	0.0473	X_{16}	0.0601
		X_{11}	0.0945	X_{14}	0.2453	VZ	0.2014
Area characteristics	0.1416	X_{17}	0.4883	X_{18}	0.0993	X_{19}	0.4124
Socio-economic conditions	0.1884	X_{20}	0.1883	X_{21}	0.6137	X_{22}	0.1980
Indirect value	0.2029	X_{23}	0.0752	X_{24}	0.5782	X_{25}	0.3466

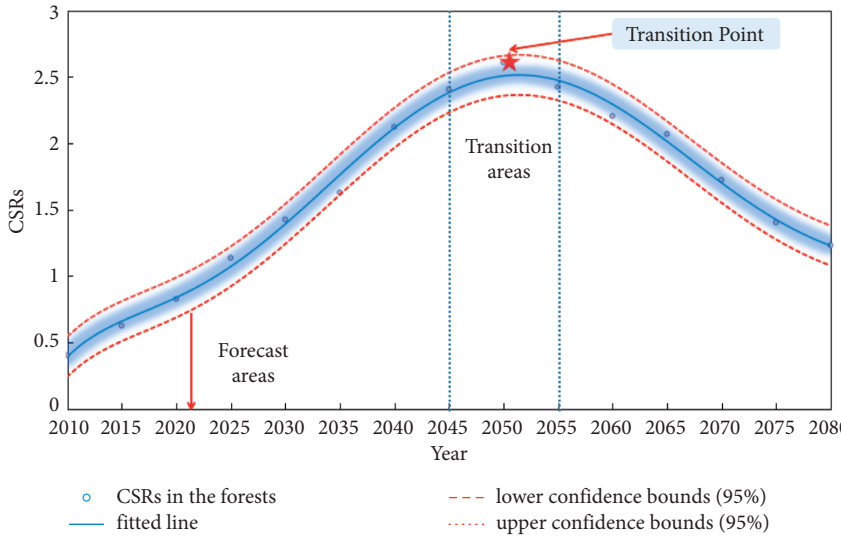

Figure 3: Fitting curve of available benefit data over time.

$$h_{ih}(k) = \sum_{i=1}^{n} w_{ih} - \theta_h, \quad h = 1, 2, \ldots, p, \tag{24}$$

$$h_{oh}(k) = f\left[h_{ih}(k)\right], \quad h = 1, 2, \ldots, p, \tag{25}$$

$$y_{io}(k) = \sum_{h=1}^{n} w_{oh} h_{oh}(k), \quad h = 1, 2, \ldots, p, \tag{26}$$

$$d_i(k) = f\left[y_{io}(k)\right], \quad h = 1, 2, \ldots, p. \tag{27}$$

The velocity of each particle is updated continuously during the training process and it is judged whether the updated velocity is greater than the maximum velocity, if it is greater than the maximum velocity, the updated velocity takes the value of the maximum velocity, otherwise, it remains unchanged. Similarly, the position of each particle is updated.

After the previous calculation the actual output can be obtained, using the actual output and the expected value can be calculated:

$$\begin{aligned} \delta_o(k) = \frac{\partial e}{\partial y_{io}} &= \frac{\partial\left\{(1/2)\sum_{i=1}^{q}\left[d_i(k) - y_{oi}(k)\right]^2\right\}}{\partial y_{oi}} \\ &= -\left[d_i(k) - y_{oi}(k)\right] y_{oi}(k), \end{aligned} \tag{28}$$

$$\begin{aligned} \frac{\partial e}{\partial w_{ho}} &= \frac{\partial e}{\partial y_{io}(k)} \Delta \frac{\partial y_{io}(k)}{\partial w_{ho}}, \\ \frac{\partial y_{io}(k)}{\partial w_{ho}} &= \frac{\partial\left(\sum_{h=1}^{p} w_{ho} h_{oh}(k) - \theta_o\right)}{\partial w_{ho}}. \end{aligned} \tag{29}$$

Calculate the fitness value for each particle:

$$f_i = \frac{1}{n_t} \sum_{q=1}^{n_t} \left(O_{iq} - T_{iq}\right)^2, \tag{30}$$

where n_t is the number of training samples;O_{iq} and T_{iq} are the actual and desired outputs of the network under the network weights and thresholds determined by the positions of the training samples at the ith particle, respectively.

Calculate the global minimum adaptation value of the particle swarm; if the current number of iterations reaches the maximum number of iterations, then the iteration stops; otherwise, calculate the individual extreme value and global extreme value position of each particle, and continue to update the velocity and position of the particles. Finally, the network weights and thresholds determined by the global pole position are output [33].

Now the trained BP neural network model can only output the normalized data, in order to get the real data, you can use the function mapminmax, the formula is as follows:

$$y = \frac{(y_{\max} - y_{\min})(x - x_{\min})}{x_{\max} - x_{\min}}. \tag{31}$$

The PSO-BP algorithm in this paper has been debugged several times to achieve the best fit for the modelling approach and to reduce errors. The final training results were obtained in Figure 4.

After several iterations, the minimum mean square error was reached with MSE = 5.0839e-08, and the best performance validation plot was obtained, as shown in Figure 5.

6.3. A Simple Case: Salonga National Forest Park. The Salonga National Park [34], located in the Zaire Nature Reserve, is situated in the central plains of Africa and covers an extensive area of 36,000 square kilometres. It is located at an altitude of 200–500 metres above sea level. Established in 1970 to protect the equatorial forest environment, it is one of the largest forest parks in the world. It is divided into two main areas, the northern and southern, and the management office is located in Montecito. The park has a wide variety of flora and fauna, and most of the Salunga National Park is covered with equatorial forest, the forests composition of which varies according to the terrain. The forest grows mainly on swamps, riversides and dry land. The land between the rivers is almost exclusively covered with semi-deciduous forest, while the riverbanks are covered with early or short-growing plants. The northern area is dense grassland (rather than savannah), which covers 0.5% of the entire area of the park.

Criterion (1): the Salonga National Park very rarely preserves the very complete ecological communities of central Africa. It also includes extensive swampy areas and forest corridor.

Criterion (2): the plants and animals in Salonga National Park are an example of biological evolution and of the adaptation of life forms to the complex equatorial rainforest environment. The sheer size of the park ensures the possibility of continued evolution of species and biomes in a relatively undisturbed forest.

6.3.1. Establishment of the Transition Points. As a result of the above feature changes in the particular forest included its location, and we make the inclusion of harvesting in its management plan, and each neuron in the hidden layer is as follows:

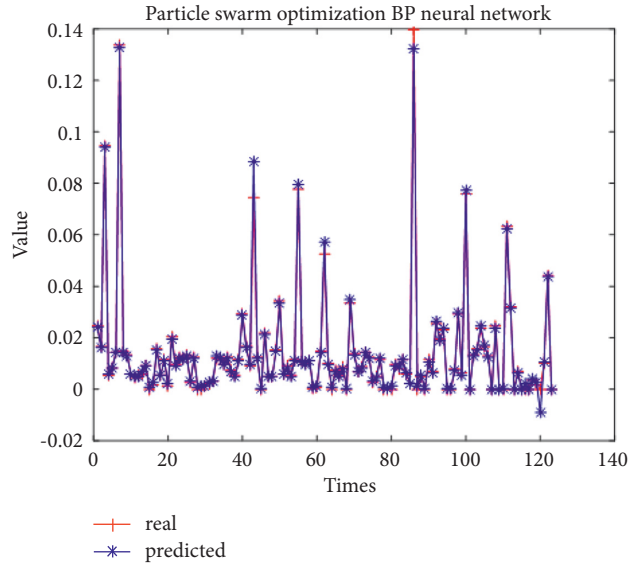

Figure 4: PSO-BP algorithm-based comparison of true and predicted values.

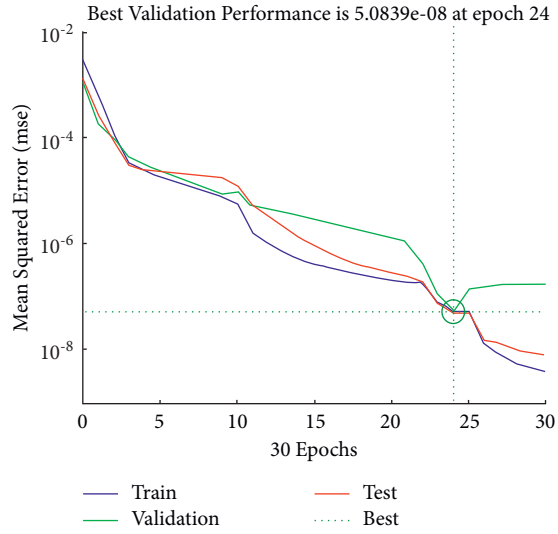

Figure 5: PSO-BP algorithm-based the best performance validation.

$$\begin{aligned}\delta_o(k) &= \frac{\partial e}{\partial h_{ih}(k)} = \frac{\partial\left\{(1/2)\sum_{h=1}^{q}\left[d_i(k) - y_{oi}(k)\right]^2\right\}}{\partial h_{ih}(k)} \\ &= \frac{\partial h_{oh}(k)}{\partial h_{ih}(k)} = -\left[\sum_{o=1}^{q}\delta_o(k)w_{ho}\right]\frac{\partial h_{oh}(k)}{\partial h_{ih}(k)},\end{aligned} \tag{32}$$

$$\begin{aligned}\frac{\partial e}{\partial w_{ih}} &= \frac{\partial e}{\partial h_{ih}(k)}\Delta\frac{\partial h_{ih}(k)}{\partial w_{ih}}, \\ \frac{\partial h_{ih}(k)}{\partial w_{ih}} &= \frac{\partial\left[\sum_{h=1}^{n} w_{ih}x_i(k) - \theta_h\right]}{\partial w_{ih}} \\ &= x_i(k).\end{aligned} \tag{33}$$

As can be seen from Figure 6, in 2049.22, when the carbon sequestration in the Salonga National Forest Park reached the peak of the CSRs, the project that does not

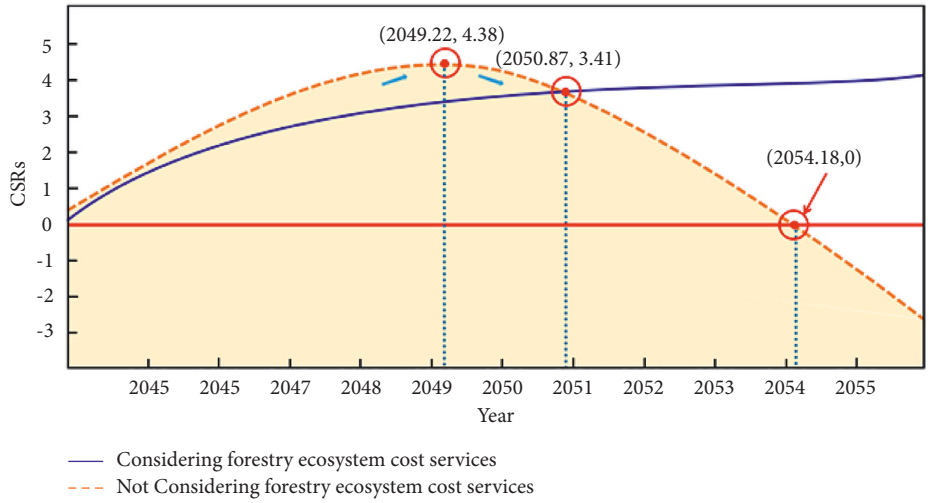

Figure 6: Determination of transition points for carbon sequestration system of the case.

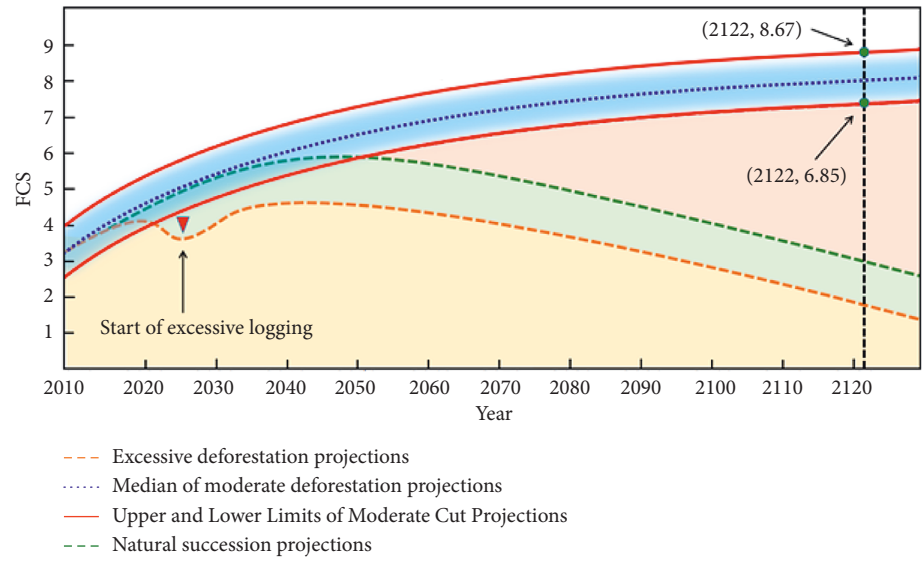

Figure 7: Projections of carbon sequestration from different forest management plans.

consider foresty ecosystem services is not implemented in an appropriate environment due to the damage to the foresty ecological environment beyond its capacity.

As a result, efficiency decreases gradually and benefit decreases rapidly with time. In 2050.87, the two curves intersect, indicating whether the benefit-cost of the foresty ecological cost service is equivalent at this time. After that, the benefits brought about by the foresty ecological service should be greater than the benefits brought from that on. When reaching 2054.18, do not consider the cost services will lead to the destruction of the ecological environment seriously affecting the project operation, so that the cost-effectiveness about the forest reach to 0.

6.3.2. DeepAR Model-Based Prediction of Carbon Sequestration. The DeepAR method based on deep learning can easily take into account features additional to the one-dimensional time series itself, and its prediction target is the probability distribution of the values taken by the series at each time step. In the particular scenario of this question, probabilistic prediction makes more sense than single-point prediction. The DeepAR algorithm may suffer from memory loss for longer time series, failing to capture information about long periods and seasons. This paper therefore incorporates a concern mechanism in the input section, using contemporaneous data as a feature:

$$v_i = 1 + \frac{1}{t_0}\sum_{t=1}^{t_0} z_{i,t}, \tag{34}$$

where$v$ is a parameter of the model and its value determines the accuracy of the model. Learn the correlation properties within different time series through deep recurrent neural networks, using multiple or multiple target numbers to improve overall prediction accuracy.

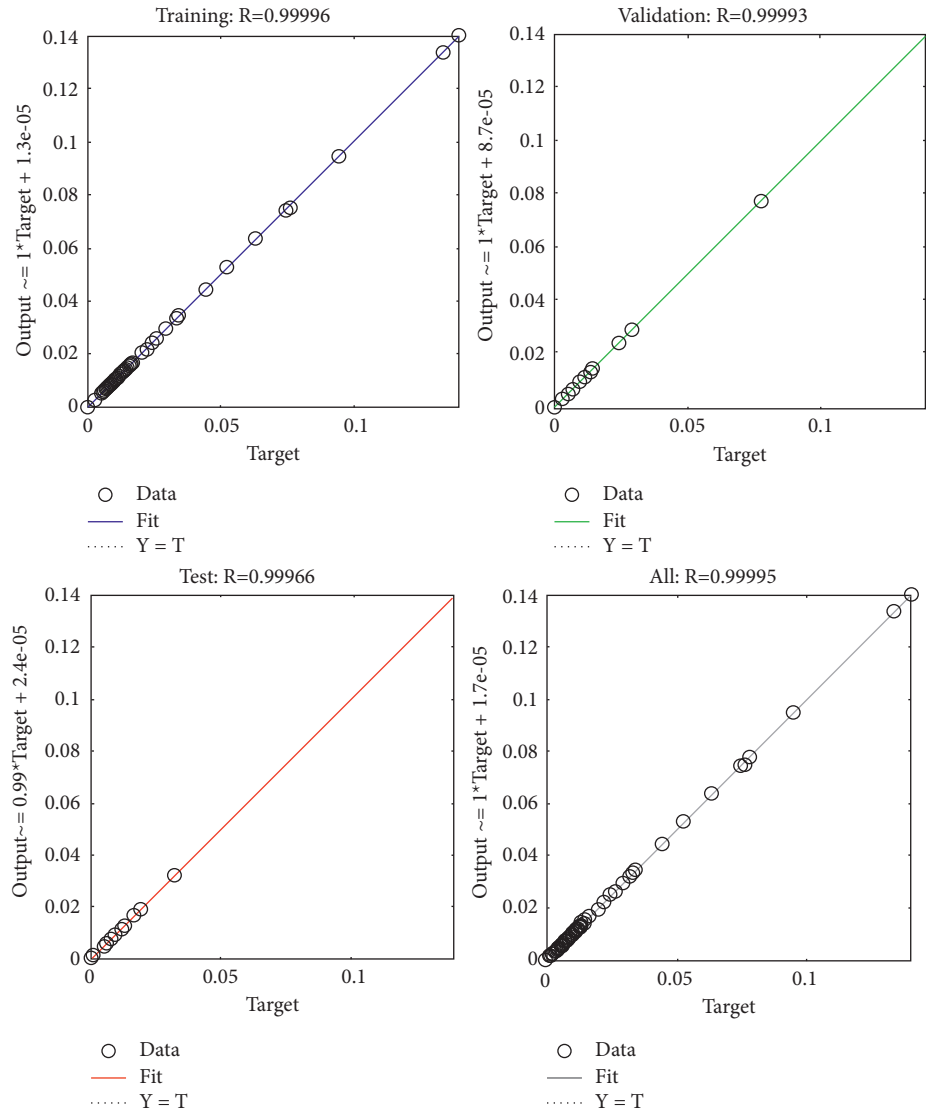

Figure 8: The training, validation, testing, and final total correlation coefficient plots.

As can be seen from Figure 7, the upper and lower limits of carbon sequestration over 100 years of the forest, as predicted by the DeepAR method, are 8.67 PgC and 6.85 PgC, respectively, after incorporating a modest rotation plan into the Salonga National Forest Park management system.

6.3.3. Result Validation. After several iterations of training, validation, and testing of the algorithm, the neural network model based on the particle swarm algorithm finally converged to the best performance validation state, and the correlation coefficient plots for the training, validation, testing, and final total training results of the neural network are shown below, respectively.

Figure 8 indicates that the training, validation, testing, and final total correlation coefficient plots for the neural network are all around 0.9999, indicating that the model fits ideally well. For the FCS model, the transition points can be determined using this particle swarm algorithm-based neural network for the final prediction [35, 36].

7. Conclusion

This paper clarifies that forest carbon sequestration is mainly influenced by three aspects: human, climate, and non-climatic physical factors, constructs a model for estimating the carbon sequestration rate of forest ecosystems based on forest age and the logistic growth equation, and combines human behaviour and climate influencing factors to make comprehensive corrections to the carbon sequestration rate of forest ecosystems per unit area. A model for calculating the carbon sequestration rate over time in a forest system was developed, which combined with the DeepAR algorithm to obtain the model of forest carbon sequestration. Then, this paper then assesses the various values of the forest, dividing the 25 factors affecting forest value assessment into five indices to establish a model of the forest ecosystem value

assessment system for application to forest value assessment under different conditions. After determining the index system, we use the EWM-CVM to integrate the indexes into the value index based on the forest ecosystem. Whereas the cost of a forest ecosystem depends to a large extent on the actual size of the area , the model's evaluation index is highest when the benefit ratio of the system is at its highest, and this is used as the effective area of the forest to propose a management plan [37, 38]. The transition point is the moment when the forest management cost and forest carbon sequestration value reach balance. This paper uses the PSO-BP algorithm to determine the transition point of forest management plan.

Data Availability

The data in this paper come from Question E of the 2022 American College Students Mathematical Modeling Competition.

Conflicts of Interest

The author declares that there are no conflicts of interest regarding the publication of this paper.

Acknowledgments

This study was funded by the Teaching and Research Fund Project of the Education Department of Anhui Province (2020jyxm0017),"First-Class Course" of Anhui University of Finance and Economics (acylkc202008) the Teaching and Research Fund Project of the Anhui University of Finance and Economics (acxkjs2021005, acyljc2021002, and acjyyb2020011).

References

[1] I.-M. Gren and A. Z. Aklilu, "Policy design for forest carbon sequestration: a review of the literature," *Forest Policy and Economics*, vol. 70, no. 1, pp. 128–136, 2016.

[2] L. F. Schulte-Uebbing, G. H. Ros, and W. de Vries, "Experimental evidence shows minor contribution of nitrogen deposition to global forest carbon sequestration," *Global Change Biology*, vol. 28, no. 3, pp. 899–917, 2022.

[3] R. Zhou, Y. Zhang, M. Peng, Y. Jin, and Q. Song, "Effects of climate change on the carbon sequestration potential of forest vegetation in yunnan Province, southwest China," *Forests*, vol. 13, no. 2, p. 306, 2022.

[4] R. K. Richards and S. Carrie, "A review of forest carbon sequestration cost studies: a dozen years of research," *Climatic Change*, vol. 63, no. 1, pp. 1–48, 2004.

[5] S. Díaz, H. Andy, and A.-W. David, "Biodiversity in forest carbon sequestration initiatives: not just a side benefit." Current," *Opinion in Environmental Sustainability*, vol. 1, no. 1, pp. 55–60, 2009.

[6] B. Sohngen and M. Robert, "An optimal control model of forest carbon sequestration," *American Journal Of Agricultural Economics*, vol. 85, no. 1, pp. 448–457, 2003.

[7] D. A. Peltzer, R. B. Allen, G. M. Lovett, D. Whitehead, and D. A. Wardle, "Effects of biological invasions on forest carbon sequestration," *Global Change Biology*, vol. 16, no. 2, pp. 732–746, 2010.

[8] R. Birdsey, K. Lucier, and L. Alan, "Forest carbon management in the United States," *Journal of Environmental Quality*, vol. 35, no. 4, pp. 1461–1469, 2006.

[9] M. A. Sutton, D. Simpson, P. E. Levy et al., "Uncertainties in the relationship between atmospheric nitrogen deposition and forest carbon sequestration," *Global Change Biology*, vol. 14, no. 9, pp. 2057–2063, 2008.

[10] S. Couture and A. Reynaud, "Forest management under fire risk when forest carbon sequestration has value," *Ecological Economics*, vol. 70, no. 11, pp. 2002–2011, 2011.

[11] R. Lal, "Forest soils and carbon sequestration," *Forest Ecology and Management*, vol. 220, no. 3, pp. 242–258, 2005.

[12] S. Belyazid and Z. Giuliana, "Water limitation can negate the effect of higher temperatures on forest carbon sequestration," *European Journal of Forest Research*, vol. 138, no. 2, pp. 287–297, 2019.

[13] V. Bellassen and S. Luyssaert, "Carbon sequestration: managing forests in uncertain times," *Nature*, vol. 506, no. 7487, pp. 153–155, 2014.

[14] J. Guo and P. Gong, "The potential and cost of increasing forest carbon sequestration in Sweden," *Journal Of Forest Economics*, vol. 29, no. 1, pp. 78–86, 2017.

[15] P. Högberg, "Nitrogen impacts on forest carbon," *Nature*, vol. 447, no. 7146, pp. 781-782, 2007.

[16] M.-E. Harmon, "Carbon sequestration in forests: addressing the scale question," *Journal of Forestry*, vol. 99, no. 4, pp. 24–29, 2001.

[17] M. Münnich Vass, "Renewable energies cannot compete with forest carbon sequestration to cost-efficiently meet the EU carbon target for 2050," *Renewable Energy*, vol. 2017, no. 107, pp. 164–180, 2017.

[18] K. Richards and K. Andersson, "The leaky sink: persistent obstacles to a forest carbon sequestration program based on individual projects," *Climate Policy*, vol. 1, no. 1, pp. 41–54, 2001.

[19] D. Wang, B. Wang, and X. Niu, "Forest carbon sequestration in China and its benefits," *Scandinavian Journal of Forest Research*, vol. 29, no. 1, pp. 51–59, 2014.

[20] M. Lal and R. Singh, "Carbon sequestration potential of Indian forests," *Environmental Monitoring and Assessment*, vol. 60, no. 3, pp. 315–327, 2000.

[21] R. Pilli, M. Vizzarri, and G. Chirici, "Combined effects of natural disturbances and management on forest carbon sequestration: the case of Vaia storm in Italy," *Annals of Forest Science*, vol. 78, no. 2, pp. 1–18, 2021.

[22] J.-M. Grünzweig, T. Lin, E. Rotenberg, and A. Schwartz, "Carbon sequestration in arid-land forest," *Global Change Biology*, vol. 9, no. 5, pp. 791–799, 2003.

[23] C. Herrero and F. Bravo, "Can we get an operational indicator of forest carbon sequestration?" *Ecological Indicators*, vol. 2012, no. 17, pp. 120–126, 2012.

[24] L. Jin, Y. Yi, and J. Xu, "Forest carbon sequestration and China's potential: the rise of a nature-based solution for climate change mitigation," *China Economic Journal*, vol. 13, no. 2, pp. 200–222, 2020.

[25] X. Tong, M. Brandt, Y. Yue et al., "Forest management in southern China generates short term extensive carbon sequestration," *Nature Communications*, vol. 11, no. 1, pp. 1–10, 2020.

[26] S. Backéus, P. Wikström, and T. Lämås, "A model for regional analysis of carbon sequestration and timber production," *Forest Ecology and Management*, vol. 216, no. 1, pp. 28–40, 2005.

[27] L. Huang, J. Liu, Q. Shao, and X. Xu, "Carbon sequestration by forestation across China: past, present, and future," *Renewable*

and Sustainable Energy Reviews, vol. 16, no. 2, pp. 1291–1299, 2012.

[28] M. Wiesmeier, J. Prietzel, F. Barthold et al., "Storage and drivers of organic carbon in forest soils of southeast Germany (Bavaria) - implications for carbon sequestration," *Forest Ecology and Management*, vol. 2013, no. 295, pp. 162–172, 2013.

[29] H.-F. Hoen and B. Solberg, "Potential and economic efficiency of carbon sequestration in forest biomass through silvicultural management," *Forest Science*, vol. 40, no. 3, pp. 429–451, 1994.

[30] Y. Malhi, P. Meir, and S. Brown, "Forests, carbon and global climate," *Philosophical Transactions of the Royal Society of London,Series A: Mathematical, Physical and Engineering Sciences*, vol. 360, no. 1797, pp. 1567–1591, 2002.

[31] R. Lal, "Carbon sequestration," *Philosophical Transactions of the Royal Society B: Biological Sciences*, vol. 363, no. 1492, pp. 815–830, 2008.

[32] J. M. Zhu, W. Y. Xia, J. J. Sun, J. B. Liu, and F. H. Yu, "The spread pattern on Ebola and the control schemes," *International Journal Of Innovative Computing And Applications*, vol. 9, no. 2, pp. 77–89, 2018.

[33] J.-M. Zhu, L. Wang, and J.-B. Liu, "Eradication of Ebola based on dynamic programming," *Computational and Mathematical Methods in Medicine*, vol. 2016, p. 9, 2016.

[34] S.-M. Zhang, W.-L. Zhan, H. Hu, Y.-S. Liu, and J.-M. Zhu, "Research on ethanol coupling to prepare C4 olefins based on BP neural network and cluster Analysis," *Journal of Chemistry*, vol. 2022, 2022.

[35] F. Xu, Y.-A. Du, H. Chen, and J.-M. Zhu, "Prediction of fish migration caused by ocean warming based on SARMA model," *Complexity*, vol. 2021, 2021.

[36] X.-W. Cai, Y.-Q. Bao, M.-F. Hu, J. B. Liu, and J. M. Zhu, "Simulation and prediction of fungal community evolution based on RBF neural network," *Computational and Mathematical Methods in Medicine*, vol. 2021, 2021.

[37] J.-B. Liu, T. Zhang, Y. K. Wang, and W. S. Lin, "The Kirchhoff index and spanning trees of Möbius/cylinder octagonal chain," *Discrete Applied Mathematics*, vol. 307, no. 22–31, 2022.

[38] J.-B. Liu, Y. Bao, W. T. Zheng, and S. Hayat, "Network coherence analysis on a family of nested weighted n-polygon networks," *Fractals. ID2150260*, vol. 29, no. 8, 2021.